NTNU

Norwegian University of
Science and Technology

Assessing the robustness of raingardens under climate change using SDSM and temporal downscaling

Guro Heimstad Kleiven

Civil and Environmental Engineering
Submission date: June 2017
Supervisor: Tone Merete Muthanna, IBM
Co-supervisor: Erle Kristvik, IBM

Norwegian University of Science and Technology
Department of Civil and Environmental Engineering

Description of Master's Thesis Spring 2017

Candidate name: Guro Heimstad Kleiven

Subject: Local climate projections / rain garden design

Title: Assessing the robustness of raingardens under climate change using SDSM and temporal downscaling

Start: 15.01.2017

Due date: 11.06.2017

Background

The city of Bergen is renowned for its plentiful rainfall. Recent reports on future climate, such as the Fifth Assessment Report (IPCC 2013) and KLIMA 2100 (Hanssen-Bauer et al., 2015), indicate an increased risk for more heavy and frequent precipitation extremes. These projections are of great concern to the city of Bergen as the infrastructure they design and manage today also should be sufficient in the future. Blue green stormwater infrastructure, like rain gardens, will have to be designed for the predicted changes in order to ensure a robust infrastructure also in the future.

The software RECARGA models water flow through a rain garden (Dussaillant et al., 2005) and can be used to study future design criteria for rain gardens. Future estimates of precipitation at the local level cannot be directly extracted from the current climate projections available through e.g. the Hanssen-Bauer et al. (2015) and IPCC (2013) reports because the spatial and temporal resolution of these projections is too coarse. In order to deal with this, downscaling techniques for translating the large-scale climate to the local scale has been developed (Maraun et al. 2010). Tools for *statistical* downscaling techniques, such as SDSM (Wilby et al. 2002), are easy to use and does not require much computer capacity or the experience of a climate researcher. In combination with temporal dowscaling (e.g. the GEV-distribution), they can be used to bridge the gap between the global climate models and local projections.

Research questions

1. To which extent can the combination of spatial downscaling with SDSM-DC, bias correction, and temporal downscaling with the GEV distribution be used to produce IDF curves for future climate in Bergen?

2. How does the applied downscaling method compare to the current practice of multiplying the design precipitation with a climate factor?

3. What is the robustness of raingardens as stormwater peak flow measures in Bergen for different future climate scenarios?

References

Benestad, R.E., Hanssen-Bauer, I. & Chen, D., 2008. *Empirical-statistical downscaling*, World Scientific.

Dussaillant, A. R., A. Cuevas, and K. W. Potter: 2005, 'Raingardens for stormwater infiltration and focused groundwater recharge simulations for different world climates'. Water Supply 5(3-4), 173–179.

Hanssen-Bauer E.J., Haddeland, I., Hisdal, H., Mayer, S., I.F., 2015. Klima i Norge 2100., (2).

IPCC, 2013. *Climate Change 2013: The Physical Science Basis. Contribution of Working Group I to the Fifth Assessment Report of the Intergovernmental Panel on Climate Change*, Cambridge, United Kingdom and New York, NY, USA: Cambridge University Press. Available at: www.climatechange2013.org.

Maraun, D. et al., 2010. Precipitation downscaling under climate change: Recent developements to bridge the gap between dynamical models and the end user. Reviews of Geophysics, 48(2009RG000314), pp.1–38.

Wilby, R. L., Dawson, C. W. & Barrow, E. M. 2002. SDSM - a decision support tool for the assessment of regional climate change impacts. Environmental Modelling & Software, 17(2), pp 147-159.

Preface

This thesis is submitted to the Norwegian University of Science and Technology (NTNU). It is a product of the course *TVM4905 Water and wastewater engineering, Master's Thesis*. The topic of the thesis is downscaling of Global Climate Models for prediction of future extreme precipitation, and application of the downscaled data for assessing the robustness of raingardens as peak flow measures under future climate change.

The study was conducted at the Department of Civil and Environmental Engineering. I would like to express my gratefulness to my supervisors associate professor Tone Merete Muthanna and PhD candidate Erle Kristvik. Kristvik has been a great support for the downscaling part. Thank you for discussing downscaling techniques with me and helping me with the programming language R. Muthanna has given me feedback and advices, especially on topics related to the raingarden assessments. I also had the opportunity to participate on the course "Statistical Downscaling of Global Climate Models using SDSM 5.2" at Smithsonian Conservation Biology Institute, Virginia, USA. Learning about downscaling and SDSM from the developers of SDSM was indeed valuable for my work.

The study was made possible in part by the EU project BINGO - *Bringing INovation to onGOing water management – a better future under climate change* and in part by Klima 2050, Centre for Research-based Innovation.

I would also like to thank:

- Post doctor Jardar Lohne for tips about paper writing
- Torstein Dalen for providing me with information on the raingarden at Bryggen, Bergen, and helping me understanding his modification of RECARGA
- Siri Foss Morken (VA-etaten, Bergen kommune), Marit Aase (VA-etaten, Bergen kommune) and Vannlaboratoriet (Bergen Vann) for conducting and analyzing infiltration tests at the raingarden at Bryggen
- Professor Arvid Næss for discussing the temporal downscaling statistics with me

Trondheim, June 8, 2017

Guro H. Kleiven

_____
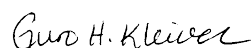
Guro Heimstad Kleiven

Sammendrag

Bergen er kjent for store nedbørsmengder. Klimaendringer er forventet å føre til enda større nedbørsmengder og høyere intensitet på de ekstreme nedbørshendelsene, noe som vil føre til mer overvann. Bedre håndtering av overvann er derfor nødvendig, og blå-grønne tiltak som regnbed kan være en løsning. Utfordringen er å estimere hvilke nedbørsmengder som må håndteres i framtiden. For å estimere dimensjonerende nedbør i fremtiden, er vanlig praksis i Norge å multiplisere dagens dimensjonerende nedbør med en klimafaktor. Alternativt kan globale klimamodeller brukes, men disse har en romlig oppløsning og tidsoppløsning som er for grov til å brukes i urban hydrologi. De globale klimamodellene kan derfor kombineres med nedskaleringsteknikker for å oppnå nødvendig oppløsning.

I dette studiet er det vurdert hvor robuste regnbed er for flomtoppsreduksjon under klimaendringer. Fremtidig nedbør ble estimert ved å bruke en metode som kombinerer romlig nedskalering og tidsnedskalering av nedbør. Til dette ble programmet the Statistical DownScaling Model - Decision Centric (SDSM-DC) og den generaliserte ekstremverdi-fordelingen (GEV-fordelingen) brukt. Resultatet av nedskaleringsprosessen var intensitet-varighet-frekvens-kurver (IVF-kurver) for historisk nedbør og nedbør som følge av mulige klimaendringer. Regnbedets yteevne ved ekstreme hendelser ble simulert i modelleringsverktøyet RECARGA for de forskjellige nedbørsscenarioene. Estimater på nedbørsscenarioene ble funnet ved å endre variansen på nedbøren og total nedbørsmengde. Endringer i varians og total nedbørsmengde var basert på Hanssen-Bauer *et al.* (2015).

Nedskaleringsmetoden ga resultater i samsvar med å gange dimensjonerende nedbør med en klimafaktor anbefalt av Norsk klimaservicesenter (2016). Altså ga den anbefalte klimafaktoren intensiteter tilsvarende det undersøkte klimascenarioet med størst nedbørsendring. For mindre komplekse systemer med lave investeringskostnader og liten risiko knyttet til svikt kan det derfor være nok å benytte anbefalt klimafaktor. Nedskaleringsmetoden ga best resultater for lengre varigheter (> 180 minutter), men bør ikke brukes for varigheter under 15 minutter. Det ble funnet at usikkerhetene fra tidsnedskaleringen var større enn usikkerhetene fra den romlige nedskaleringen. Metoden egner seg best for å demonstrere mulige scenarioer som følge av ulike klimaendringer, til å stressteste systemer av interesse og/eller være del av en risikoanalyse.

Resultatene viser at regnbeds robusthet, når det gjelder å håndtere flomtoppen fra overvann under klimaendringer, er svært avhengig av mettet hydraulisk konduktivitet (K_{sat}). De

oppnådde resultatene viser at en høyere K_{sat} er gunstig for å redusere overløp og for å øke fordrøyningstiden. Basert på dette, er en høyere K_{sat} enn hva som er tidligere anbefalt for kaldt klima nødvendig for at regnbed skal være robuste under klimaendringer. Derimot er gir en lavere K_{sat} høyest flomtoppsreduksjon. Derfor bør mediet regnbedet er bygd opp av (og med dette K_{sat}) bestemmes ut i fra hvilke egenskaper man ønsker at regnbedet skal ha. En løsning som kombinerer ulike egenskaper, for eksempel ved å ha ulike regnbed/infiltrasjonsløsninger i serie, vil likevel gi størst robusthet.

Table of contents

Thesis structure

The thesis has an untraditional format in the sense that a paper is the main product. The paper has been submitted to the International Water Association (IWA) journal *Water Science and Technology*, but is yet not published. A manuscript of the paper ("Assessing the robustness of raingardens under climate change using SDSM and temporal downscaling") is therefore the main content of the thesis. Further information about the work, and results not included in the paper, are found in 0 - Appendix D.

The work will be presented at the conference *Embrace the Water* in Gothenburg, Sweden, 12th of June 2017. The poster which will be used for the presentation, can be accessed using the QR code in Appendix E.

Much of the thesis work was conducted using the programming language R. One of the R scripts is attached in Appendix F, while the rest of the applied scripts can be accessed at Daim (https://brage.bibsys.no/xmlui//handle/11250/223328).

x

Abbreviations

AM	Annual Maximum
CSO	Combined Sewer Overflow
DDF	Depth Duration Frequency
GCM	Global Climate Model
GEV	Generalized Extreme Value
IDF	Intensity Duration Frequency
IVF	Intensitet-varighet-frekvens
MET	Meteorologisk Institutt (Norwegian Meteorological Institute)
MLE	Maximum Likelihood Estimation
MPD	Modified Philip-Dunne
NCEP	National Centers for Environmental Prediction
NCM	Non-Central Moments
RCP	Representative Concentration Pathway
SDSM-DC	Statistical DownScaling Model - Decision Centric

Assessing the robustness of raingardens under climate change using SDSM and temporal downscaling

Guro Heimstad Kleiven

Department of Civil and Environmental Engineering, The Norwegian University of Science and Technology (NTNU), 2017

Abstract

Climate change is expected to lead to higher precipitation amounts and intensities. This study was carried out to (1) estimate the future precipitation extremes in Bergen (Norway) and (2) assess the robustness of raingardens as stormwater peak flow measures.

A combined spatial temporal downscaling method using the Statistical DownScaling Model-Decision Centric (SDSM-DC) and the Generalized Extreme Value (GEV) distribution was applied to estimate future precipitation. Raingarden performance was simulated with the modelling tool RECARGA.

The method gave results similar to multiplying with a climate factor as recommended by Norsk klimaservicesenter (2016). Uncertainties were found to be higher from temporal rather than spatial downscaling. The method is best suited as a tool for demonstrating possible climate change scenarios, and stress testing systems of interest. The robustness of raingardens as stormwater peak flow measures was found to be highly dependent on saturated hydraulic conductivity (K_{sat}). The results obtained indicate that a higher K_{sat} is beneficial for reducing overflow and increasing lag time. However, a lower K_{sat} value achieves the highest peak flow reductions.

According to the research, a higher K_{sat} than what is earlier recommended for cold climates is needed to make raingardens robust under climate change.

1. Introduction

The Damsgård area (Bergen, Norway) is prone to high amounts of runoff, coming from the urbanized area itself and the hillsides upstream the urban development. Damsgård drains to the small fjord Puddefjorden (Figure A.1), resulting in combined sewer overflows (CSOs) to the fjord during heavy precipitation events.

Bergen is renowned for its plentiful rainfall, with an annual mean of 2250 mm (Jonassen *et al.* 2013). Climate change is expected to lead to higher precipitation amounts, and more frequent storm events with higher intensities in the future (Hanssen-Bauer *et al.* 2015). This can lead to increased number of CSOs (Nilsen *et al.* 2011). Solutions to reduce the stormwater runoff from Damsgård are therefore needed. Blue green stormwater infrastructure, like raingardens, have been pointed out to be beneficial measures for climate change mitigation (e.g. Demuzere *et al.* 2014). This is amongst other factors because of their ability to significantly remove peak flow runoff (e.g. Hunt *et al.* 2008).

For estimating future design rainfall intensity, a common practice in Norway today is simply to apply a climate factor (a percentage safety factor) to present precipitation. Frequently asked questions by the designers concern the magnitude of the climate factor and whether simply multiplying today's design precipitation with a climate factor is sufficient. An alternative approach is applying General Circulation Models (GCMs), which simulate the future climate scenarios on a global scale. These models are, however, too coarse to reproduce detailed climate predictions at the temporal and spatial scale necessary for hydrological assessments (Herath *et al.* 2016). Therefore, to translate the large-scale climate to the local scale, downscaling techniques can be applied. *Statistical* downscaling is a downscaling approach that utilizes statistical relationships between the large-scale climate (predictor) and the local climate (predictand) to simulate the climate at a local scale (Benestad *et al.* 2007).

Several authors (e.g. Nilsen *et al.* 2011) maintain that the main uncertainties in climate change studies stem from the emission scenarios and the capacity of the GCMs to represent the climatic consequences of these. In addition to these, there are uncertainties in the downscaling procedure. Possible outcomes of climate change might in this manner be missed by applying the GCMs blindly. Some researchers (Wilby and Dessai 2010; Brown and Wilby 2012; Yates *et al.* 2015) are therefore suggesting an alternative approach for assessing the risk connected to climate change. This includes using the GCM projections to inform the analysis, rather than drive them, and to use the information to stress test the investigated system. In this way, greater emphasis is placed on the investigated system itself and possible adaption choices (Yates *et al.* 2015).

The software The Statistical DownScaling Model - Decision Centric (SDSM-DC) (Wilby *et al.* 2014) facilitate the above-mentioned use of GCMs. The output from SDSM-DC is

limited to one day. However, for the results from the downscaling to be useful for evaluation of raingardens and other hydrological assessments in urban watersheds, a higher temporal resolution is necessary (Herath *et al.* 2016). Common practice is applying Intensity Duration Frequency (IDF) curves for design of urban stormwater systems. In this study, SDSM-DC was combined with a temporal downscaling approach using the Generalized Extreme Value (GEV) distribution (Nguyen *et al.* 2002) to obtain IDF curves for future climate change scenarios for Bergen, following the procedure of Nguyen *et al.* (2007).

Based on the above, this paper addresses the following research questions:

1. To which extent can the combination of spatial downscaling with SDSM-DC, bias correction, and temporal downscaling with the GEV distribution be used to produce IDF curves for future climate in Bergen?
2. How does the applied downscaling method compare to the current practice of multiplying the design precipitation with a climate factor?
3. What is the robustness of raingardens as stormwater peak flow measures in Bergen for different future climate scenarios?

2. Methods

The method was divided into three steps; (1) a spatial-temporal downscaling approach to obtain local extreme rainfall for construction of IDF curves from large-scale climate variables according to the prescriptions of Nguyen *et al.* (2007) (Figure 1); (2) construction of IDF curves using observed precipitation data and the climate factors 1.2 and 1.4; and (3) simulations of raingarden performance in RECARGA with design storm events constructed form the developed IDF curves.
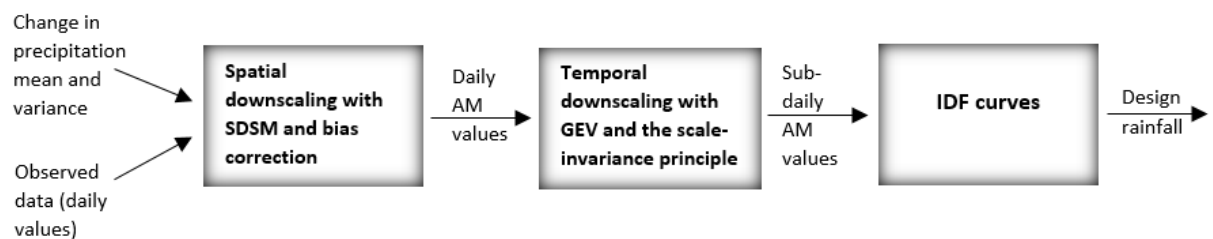

Figure 1 Flow chart describing step 1 in the method. AM is an abbreviation for "annual maximum".

2.1.   Collection of precipitation data

Observed precipitation data was used for two purposes: (1) Calibrating the SDSM-DC and statistically downscale from global to local climate with SDSM-DC, and (2) developing IDF curves from (i) observed data and (ii) downscaled climate data using temporal downscaling.

The weather stations were chosen on basis of proximity to the study site. The longest record of daily precipitation in the area was found at The Norwegian Meteorological Institute's (MET) station at Florida, Bergen (50540). Thirty years of data (1985 – 2015) from this station was used for calibration and validation of the SDSM-DC model. However, this station has only four years of sub-daily precipitation data. A station seventy meters away, Florida UIB (50539), has minute data for 10 years (see Figure A.2). This station was therefore chosen for providing the sub-daily precipitation.

The data has been quality controlled by MET and downloaded from eklima.no.

2.2.   Downscaling of precipitation

The spatial-temporal downscaling is a combination of separate spatial and temporal downscaling techniques. It uses SDSM-DC to link the large-scale climate to the local climate and make future climate estimates. The results are further bias corrected. The temporal downscaling approach uses the scaling concept and the GEV distribution to obtain a relationship between daily and sub-daily precipitation (Nguyen *et al.* 2002). The GEV distribution is also used to derive IDF curves. The SDSM-DC and the GEV distribution have been applied successfully in combination to develop IDF curves (e.g. Nguyen *et al.* 2010; Herath *et al.* 2016).

The methods for spatial, including bias correction, and temporal downscaling described by Nguyen *et al.* (2007) and Herath *et al.* (2016) was used with the following exceptions (for detailed description about the downscaling method, see B.1. and B.2.):

2.2.1. Scenario generation

SDSM-DC does not include GCMs directly, but the user of the model can apply scenarios for the future climate by changing *occurrence, mean, variance* and *trend* of e.g. the precipitation (Wilby *et al.* 2014). To assess the effects of higher amounts and intensity of rainfall, changes in the treatments mean and variance were investigated by adding expected (1) *change (%) in total precipitation amounts* and (2) *change (%) in precipitation amounts*

at days with heavy precipitation to the SDSM-DC time series respectively (Table 1). (1) and (2) are estimates of the expected changes from 1971-2000 to 2071-2100 for the whole Sunnhordland region (Hanssen-Bauer *et al.* 2015).

Table 1 Estimates on how the precipitation mean and variance might change.

Climate Scenario	0	1	2	3	4	5	6
Changes based on	Observed	RCP 4.5 low	RCP 8.5 low	RCP 4.5 med	RCP 8.5 med	RCP8.5 high	RCP8.5 high autumn/winter
MEAN: Change in total precipitation amounts (%)	0	0	2	6	12	20	30
VARIANCE: Change in precipitation amounts on days with heavy precipitation (%)	0	2	8	7	14	21	30

The climate scenarios 1-5 were based on yearly values. Climate scenario 6 was based on the worst combination of seasonal values. Annual values for RCP4.5 High (12, 12) and RCP 8.5 Med (12, 14) were quite similar. Therefore, only a change corresponding to RCP 8.5 Med was investigated.

2.2.2. Temporal downscaling

There are several ways of estimating the GEV parameters, where non-central moments (NCMs) have been used with this approach before (e.g. Nguyen *et al.* 2010; Herath *et al.* 2016). However, due to a combination of applicability and study scope, the maximum likelihood estimation (MLE) method was used for parameter estimation in this study. The chosen parameters are those which maximize the log-likelihood function, which is given as (Coles 2001):

$$l(\theta) = \sum_{i=1}^{N} \log g\ (z_i; \theta) \tag{1}$$

where g is the probability density function of the GEV distribution. $\theta = [\xi,\ \mu,\ \sigma]$. ξ, μ and σ are the shape, location, and scale parameter of the GEV distribution.

The scaling factors for the different parameters were found as described by Nguyen *et al.* (2007) and Herath *et al.* (2016). They were further plotted against precipitation duration

with the aim of finding one common scaling factor. This was calculated by finding the mean of the derived scaling factors.

For constructing depth duration frequency (DDF) curves, the return levels (z_p) were calculated (Coles 2001):

$$z_p = \mu - \frac{\sigma}{\xi}\left[1 - \{-\log(1-p)\}^{-\xi}\right], \text{ for } \xi \neq 0 \tag{2}$$

where $G(z_p) = 1 - p$, and z_p are associated with the return period $\frac{1}{p}$. To get IDF curves, the return values were converted from mm to mm/hr. These intensities were plotted against the precipitation durations.

2.3. Construction of IDF curves for observed data

An IDF curve for observed historical precipitation was developed using the GEV distribution. The intensities were multiplied by the climate factors 1.2 (a commonly used climate factor) and 1.4 (Norsk klimaservicesenter 2016). A second IDF curve for observed historical precipitation was constructed using the derived scaling factors for comparing purposes.

2.4. Raingarden assessments

2.4.1. Infiltration rate

It was assumed that a possible raingarden at Damsgård will have the same size relative to the watershed (6%) and the same watershed characteristics as an existing raingarden located at the close-by site Bryggen (the city center of Bergen). The robustness of the raingarden was assessed by investigating the performance with different infiltration rates, represented by the saturated hydraulic conductivity (K_{sat}). The raingarden was tested with three different K_{sat}: 38 cm/h, 10 cm/h and 3.4 cm/h. The high K_{sat} of 38 cm/h was the value from the existing raingarden at Bryggen, obtained by Modified Philip-Dunne (MPD) infiltration tests, as described by Ahmed *et al.* (2014). Paus *et al.* (2016) found 10 cm/h to be the minimum recommended K_{sat} in cold climates. They further found that K_{sat} during autumn/early winter (i.e. September to December) was 25-43% of summer infiltration, with a mean of 34%. Therefore, 3.4 cm/h represented the winter infiltration.

2.4.2. Evaluating performance

The performance was evaluated based on (1) overflow (% of runoff into the raingarden), (2) change in lag time (change in minutes compared runoff without raingarden), and (3) flow peak reduction in underdrain compared to incoming runoff (%). Lag time is in this

study defined as the time from the rainfall event starts until flow peak of runoff or flow peak in the underdrain is reached.

2.4.3. Simulation in RECARGA

RECARGA models the performance of a raingarden in 1D vertical flow direction (Dussaillant *et al.* 2005). The model applies Green-Ampts (Mein and Larson 1973) and a surface water balance to model infiltration, runoff and evapotranspiration, and Genuchtens equations (Van Genuchten 1980) to model percolation between the model's three soil layers.

A modified version of RECARGA, allowing for minute resolution for input and output was used for the simulations (Dalen 2012). Using RECARGA, the performance with the different K_{sat} values was tested for the obtained climate scenarios (see Table C.1 for the input to RECARGA).

2.4.4. Creation of time series

RECARGA requires time series as input. These were made by symmetrical hyetographs with one hour duration, and calculation steps adapted to the developed IDF curves. As it is unlikely to have no precipitation prior to or following an extreme event, two days of uniformly distributed rainfall, equaling the average daily rainfall, were included before and after the event. Doing this also accounted for initial water in the soil and for delays in runoff and infiltration.

3. Results and discussion

The accuracy and applicability of the method was assessed by investigating the performance of each step separately and combined.

3.1. Spatial downscaling

The predictors shown in Table 2 were chosen based on assessments of scatter plots, correlation matrices and p-values. The goodness of fit of the model was assessed by the explained variance (R^2). The model had an average $R^2 = 0.22$ (Table D.1). This is comparable to previous studies (Mahmood and Babel 2013; Herath *et al.* 2016). Wilby *et al.* (2002) argue that an R^2 under 0.4 is likely for precipitation occurrence and amounts. Further, the average cross validation $R^2 = 0.20$. The two R^2 values being close, indicates that the model performs well. The model performs best in autumn/winter, with the highest R^2 in September (0.26). The poorest performance is found during summer ($R^2 = 0.11$ in

July). The climate patterns might explain the difference. The precipitation in Bergen is in general governed by the topography and westerly winds from the North Sea (Jonassen *et al.* 2013). However, the precipitation during summer is typically influenced by convective processes, which are local phenomena. The model appears to reflect the large-scale patterns well, while being less successful at capturing variations due to local conditions.

Table 2 The chosen National Centers for Environmental Prediction (NCEP) predictor variables.

Parameter code	Description
Mslp	Mean sea level pressure
p5_f	Geostrophic airflow velocity at 500 hPa
p8_f	Geostrophic airflow velocity at 850 hPa
p8_u	Zonal velocity component at 850 hPa
p850	850 hPa geopotential height

3.2. Bias correction

Figure 2 shows that the SDSM-DC simulated daily annual maximum (AM) rainfall was overestimated for most years, and underestimated for the extreme years. This applies to some extent after bias correction too, though it is highly improved. Further, root-mean-square deviation (RMSE) improved from 8.14 mm to 4.19 mm, and the Nash-Sutcliffe efficiency coefficient (N-S) improved from 0.85 to 0.96 due to bias correction. The percentage bias (p-bias) improved from 7.20% to 0% (Table D.2).
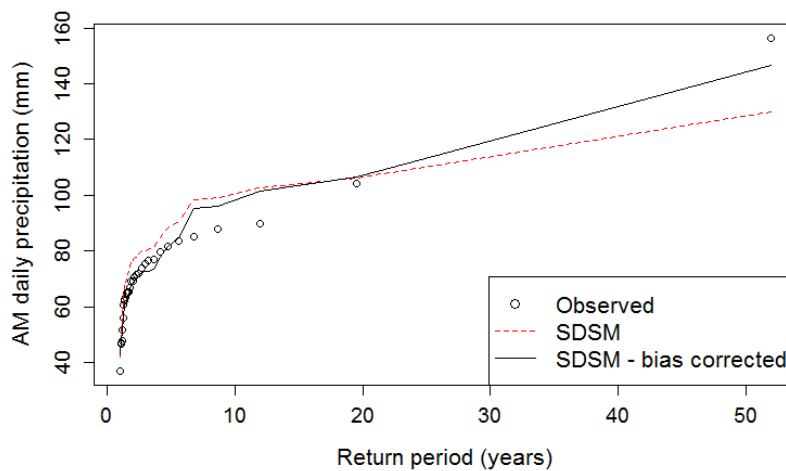

Figure 2 Historical AM daily precipitation values based on observed data, SDSM results and bias corrected SDSM results.

3.3. Temporal downscaling

The scaling factor β was 0.472. When deriving the scaling factors, it was found that the scaling factors for all durations except for 12 hours were similar for all return periods (Figure D.3). Therefore, the 12-hour duration was excluded in the calculation of a common scaling factor (Figure D.4). The reason for the diverging scaling factor at 12-hour duration is that the daily data follows MET's definition of a day (7.00 am to 7.00 am). The sub-daily durations were derived from observed minute data. While aggregating this data, a day was considered midnight to midnight. This difference may have influenced the data for the 12-hour durations. However, when comparing the observed IDF curves found directly from the data and by using the scaling factor, it is seen that the longest durations are well represented by the scaling IDF curve (Figure 3a).
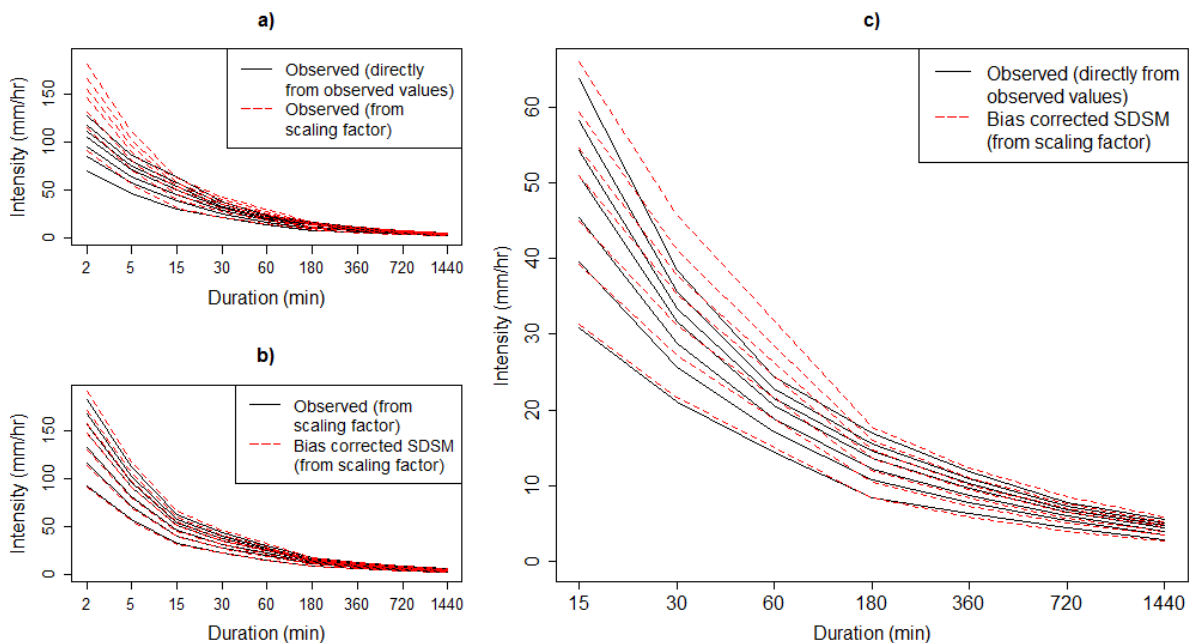
Figure 3 IDF curves showing the ability of the applied method to represent historical precipitation intensities. a) observed precipitation, derived directly from the observed values, and by using the scaling factor; b) observed and bias corrected SDSM precipitation, both developed using the derived scaling factor; c) observed precipitation found directly from observed values and bias corrected SDSM precipitation found by using the scaling factor. The return periods are 2, 5, 10, 20, 30, 50 and 100 years.

Figure 3a also shows that using the scaling procedure leads to high overestimation of the intensity for the shortest durations (< 15 minutes). This implies that the scaling principle should not be used for these intensities. The finding corresponds to Herath *et al.* (2016) who downscaled to 30 minutes at the lowest. Nguyen *et al.* (2010), on the other hand, used a downscaled resolution of five minutes in further hydrological assessments. The temporal scaling procedure represents the durations over 180 minutes well (Figure 3a). The longest durations being best represented is not surprising, as one could expect a closer statistical relationship between e.g. AM three-hour precipitation and AM daily precipitation than AM 15-minute precipitation and AM daily precipitation. For durations between 15 and 180 minutes, the intensities for the higher return periods are overestimated. The 15-minute duration was chosen as lowest duration in the IDF curves in this study. In addition, only intensities over 15 minutes were further used in the RECARGA simulation.

The GEV parameters were estimated using maximum likelihood estimation (MLE) because MLE is a widely used approach for parameter optimization (Scholz 2006). The study aims to investigate tools that are available for the end-users. Using a well-known, standard method like MLE was therefore considered beneficial. Based on the results from this study, using MLE gave good fit to the observed data (see Figure D.2) and acceptable results from the temporal downscaling (see discussion above). Nevertheless, is the temporal downscaling step identified as the major source of uncertainty (see Figure 3 and section 3.4). Future studies investigating whether another method for parameter estimation, like NCMs as suggested by Nguyen *et al.* (2002), performs better would therefore be beneficial.

3.4. Combination of spatial and temporal downscaling

Figure 3b shows that the accuracy of the spatial downscaling (after bias correction) applies for sub-daily intensities as well as for daily precipitation. The spatially downscaled IDF curve follows the same pattern as the IDF curve based on observed data when both curves are constructed using the derived scaling factor. However, the fit is best for the lower return periods.

Figure 3c shows that the same patterns as described in the section 3.3 applies for the spatially and temporally downscaled IDF curve. The small overestimation for larger return periods in the spatial downscaling step (Figure 3b) carries over to the spatially and temporally downscaled IDF curves (Figure 3c), though the temporal downscaling is the main source of inaccuracy in the results.

3.5. Comparison between the downscaled scenarios and climate factors

The IDF curves for the chosen scenarios were compared to applying the climate factor 1.4, which is the recommended climate factor for durations less than three hours for Hordaland county (Norsk klimaservicesenter 2016), and to applying the commonly used climate factor of 1.2. The comparison is shown for the 20-year return period (Figure 4), which is the design criteria for stormwater pipes in the city of Bergen (Bergen kommune 2005). Applying the climate factor of 1.4 results in intensities higher than all the investigated climate scenarios for all durations, except for the durations from 30 to 120 minutes. Knowing that the spatially and temporally downscaled intensities are overestimated for these same durations (Figure 3c), the 1.4 climate factor gives the highest safety margin amongst the investigated cases. The intensities given by the commonly applied climate factor of 1.2 on the other hand, are exceeded by several of the climate scenarios for durations under 180 minutes. For durations over 180 minutes, is it only exceeded by climate scenario 6. This indicates that a lower climate factor might be used for longer durations. However, the shorter durations are of most interest in design of stormwater infrastructure (Herath *et al.* 2016; Nilsen *et al.* 2011).
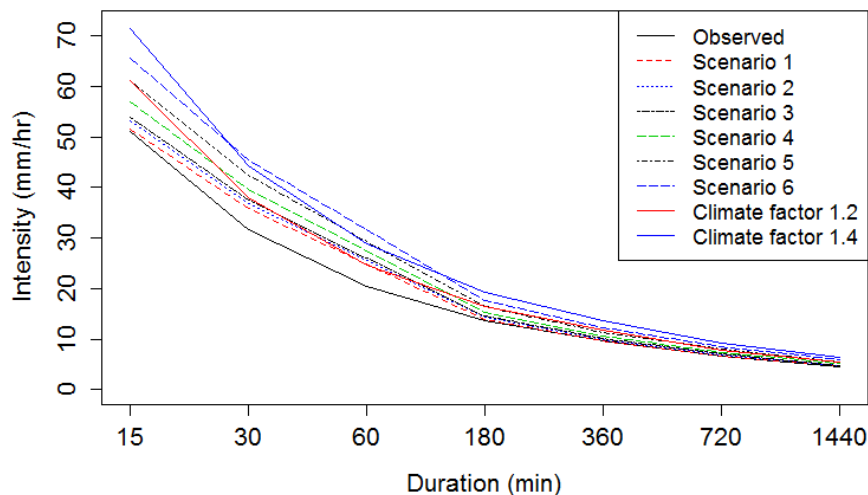

Figure 4 IDF curve for all investigated cases for return period 20 years.

Even though the climate factor 1.4 gives the highest safety margin in this study, it is important noticing that this does not mean that applying this climate factor always is sufficient. The investigated scenarios do not constitute an upper limit for climate change.

11

The uncertainties of future emission scenarios, the GCMs and the spatial and temporal downscaling procedure make it crucial to use the results cautiously. This is the motivation behind the SDSM-DC. The GCMs can be used to inform the analysis, but they are not driving them (Wilby *et al.* 2014). This is done by selecting treatments to apply to the current climate situation. In this study, the GCM output was used to inform the choice of treatments, as recommended by Brown and Wilby (2012). The annual and seasonal change estimates for the Sunnhordland region represented the climate changes.

One should also be aware of that SDSM-DC downscales the climate before the treatments are applied. The climate treatments are therefore not downscaled. Thus, the changes for Bergen might be higher or lower than implied by the applied changes. Furthermore, is the *change (%) in rainfall amounts at days with heavy precipitation* applied as an estimate of the treatment *variance*.

The applied treatments are from Hanssen-Bauer *et al.* (2015) and the 1.4 climate factor is from Norsk klimaservicesenter (2016), which is based on Hanssen-Bauer *et al.* (2015). Thus, the climate factor and the applied treatments are based on the same GCM output. One could therefore expect that multiplying with the 1.4 climate factor would give similar intensities as the worst climate scenario. This was indeed the case, which indicates that there is an agreement between the downscaling approach used in this study and the downscaling methods used by Hanssen-Bauer *et al.* (2015).

3.6. The raingarden as peak flow measure

The raingarden performance was assessed for a 20-year storm because this is the design storm for stormwater pipes in the city centre of Bergen (Bergen kommune 2005). However, it can be argued that it is not reasonable to design raingardens for capturing all the runoff from such a rather large event. Raingardens are recommended to be designed to capture the "everyday" runoff, and to be combined with safe flood ways for larger events (Paus and Braskerud 2014). Therefore, infiltrating 80% of the incoming runoff is considered a successful performance in this study. With concern to Puddefjorden, the risk of a CSO every 20th year caused by 20% of the runoff from Damsgård is well within acceptable risk levels.

K_{sat} = 38 cm/h was the only investigated infiltration rate that gave under 20% overflow for all climate scenarios (Figure 5a). It was further found that the K_{sat} should be over 17 cm/h to infiltrate 80% of the runoff for today's condition. However, to meet the criterium for all

the investigated climate scenarios, it should be at least 33 cm/h. In addition, should winter conditions also be accounted for. A reduction of K_{sat} 33 cm/h to e.g. 11.2 cm/h (34% reduction, see section 2.4.1), would neither today nor in the future will give adequate infiltration.
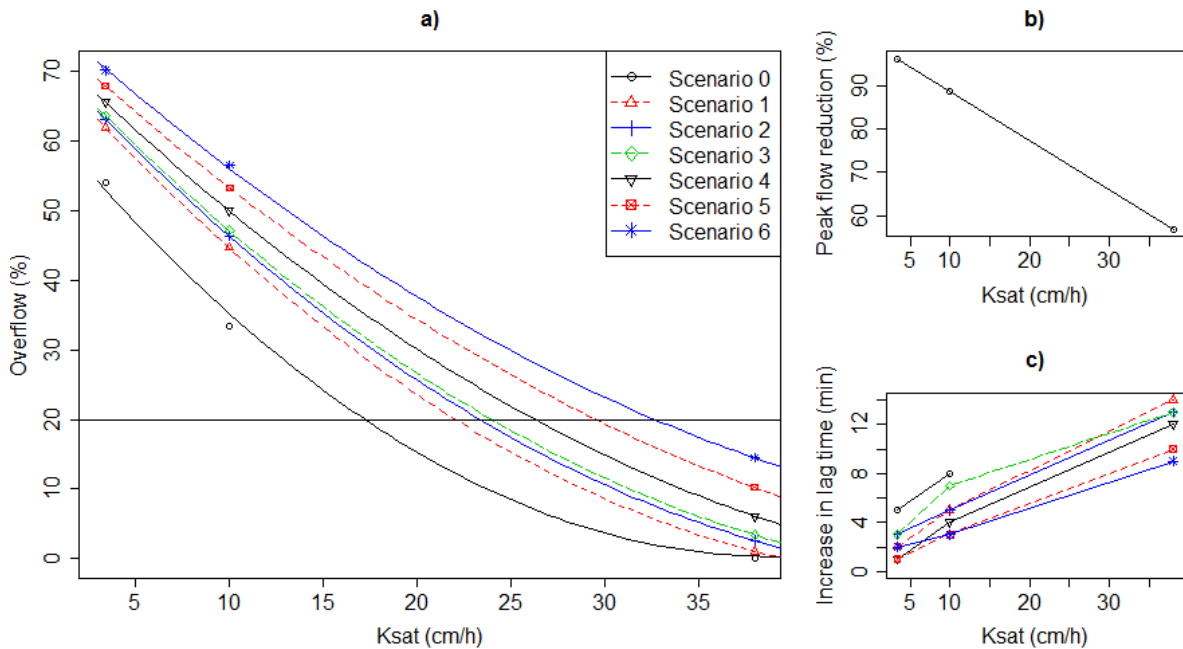

Figure 5 Performance of the raingarden for different K_{sat} values for the investigated climate scenarios. a) Percentage of incoming runoff becoming overflow from the raingarden (%); b) peak flow reduction compared to peak flow without raingarden (%); c) lag time reduction for peak overflow from the raingarden compared to peak runoff without raingarden (min).

For all investigated K_{sat} values, the peak flow in the underdrain was reached before the peak runoff from the event. Hence the lag time was reduced for the flow in the underdrain compared to the lag time without a raingarden. However, an increase in lag time for overflow from the raingarden compared to the pre-raingarden conditions was observed. The largest increase was found for a $K_{sat} = 38$ cm/h, ranging from nine minutes for climate scenario 6 to 14 minutes for climate scenario 1 (Figure 5c). A $K_{sat} = 3.4$ cm/h gave the lowest increase in lag time, ranging from one to three minutes for the different climate scenarios and five minutes for today's situation.

The peak flow reduction was only dependent on K_{sat}, and was independent of the climate scenarios (Figure 5b). The highest peak flow reduction was found for $K_{sat} = 3.4$ cm/h (96%), while the lowest was found for $K_{sat} = 38$ cm/h (57%).

13

Thus, it is seen that a higher K_{sat} results in less overflow, and an increase in overflow lag time, whereas a lower K_{sat} is the most efficient for reducing the peak flow. Nevertheless, even though a higher peak flow reduction in the underdrain is achieved with a lower K_{sat}, does a lower K_{sat} also lead to more overflow. Thus, with a low K_{sat} value will only infiltration of the first runoff from a rainfall event (i.e. first flush) be achieved. Alternatively, is a larger storage volume on the top of the raingarden is necessary to reduce the overflow.

The results show that the choice of filter medium (and ultimately K_{sat}) should be based on whether peak flow reduction or detention is the most important objective. Nevertheless, might a combination of different solutions be beneficial. One could e.g. have a series with a high-infiltration rate raingarden first, draining into another raingarden or infiltration-based solution with lower infiltration capacity. Or, the raingardens could be placed in opposite order, with a low-infiltration rate raingarden first, infiltrating the small events and the first flush for larger events, and then overflowing to a second raingarden/infiltration-based solution with higher infiltration rate. The above are two possible solutions, illustrating that the key to increased robustness is a combination of solutions.

3.7. Overall performance of method

The study shows that the different climate scenarios give highly different design events (Figure 4), and thus requirements for a raingarden to be well-performing (Figure 5). As discussed, the climate scenario selection, but also the applied downscaling procedure are sources of uncertainties. This was demonstrated by simulating a design event derived by multiplying the observed 20-year return period intensity with the climate factor 1.4 in RECARGA. It was seen that for $K_{sat} = 38$ cm/h, the 1.4 climate factor gave the highest percentage overflow, even though the precipitation volume for climate scenario 5 (29.38 mm) and 6 (32.00 mm) were higher than for the climate factor 1.4 (28.75 mm). For $K_{sat} = 10$ cm/h on the other hand, the downscaled climate scenarios always gave the highest overflows. This might be due to the shapes of the IDF curves. The climate factor IDF curves had higher intensity for the short durations than the climate scenario IDF curves (Figure 4). Because of the high infiltration rate with $K_{sat} = 38$ cm/h, only the most intense minutes gave overflow. The infiltration rate is lower with $K_{sat} = 10$ cm/h. Therefore, the lower intensities also resulted in overflow volume. As these intensities were higher in the climate scenario IDF curves, it generated more overflow volume compared to the climate factor IDF curve.

The results obtained from the downscaling and simulation in RECARGA must be used with care. The applied downscaling method is a good tool for showing the range of possible outcomes of climate change. Generally, it can be used to stress test systems for possible climate change scenarios, and to evaluate the response of an investigated system, as suggested by Wilby *et al.* (2014). In a design perspective, one should always consider the risk associated with failure of the system (Hanssen-Bauer *et al.* 2015). The common understanding of risk is a combination of probability and consequence. The applied downscaling method can be used together with other simulation tools, e.g. hydrological or hydraulic, to indicate the probability of an event occurrence. The combination of these results and the consequence of an event can be used to estimate risk connected to the event. From this, the best design or adaption measure can be decided.

The method used in this study is a comprehensive process suited for cases with high investment costs and high consequences due to failure. It can therefore be suggested that the simpler approach of applying a climate factor is adequate for systems with smaller investment costs and lower consequences due to failure. According to the results, the recommended climate factor for durations under three hours would be 1.4 at the study site, as suggested by Norsk klimaservicesenter (2016).

4. Conclusions

A combination of spatial and temporal downscaling was applied to make historical and future IDF curves for Florida (Bergen, Norway), and assess the robustness of raingardens as peak flow reduction measures under climate change. The climate change scenarios were generated by manipulating the mean precipitation and precipitation variance.

The IDF curves developed by using the downscaling method represent the lowest return periods well, but are inaccurate for the highest return periods. Further are durations over 180 min best represented, while durations under 15 min are overestimated. It was found that the largest inaccuracy in the downscaling procedure was the temporal downscaling step. More research should be done on improving this step.

Applying the climate factor recommended by Norsk klimaservicesenter (2016) (1.4 for durations under three hours at the study site) seems sufficient for less complex systems with small investment costs and low consequences due to failure. However, for more complex systems with higher consequences due to failure, making use of the method applied in this study will be beneficial. Nevertheless, use of the method should be restricted

15

to stress testing of systems of interest and/or being part of a risk analysis. More work should be carried out to reduce the uncertainties connected to climate change estimations.

The robustness of raingardens as stormwater peak flow measures is highly dependent on the K_{sat} value. The higher K_{sat} value, the more robust as a stormwater peak flow measure the raingarden will be, both in terms of overflow, and lag time. Based on overflow and lag time, the recommended minimum K_{sat} value for cold climates of 10 cm/h is insufficient. However, even though a lower K_{sat} results in higher overflow, the peak flow reduction of the infiltrated water is highest for these K_{sat} values. It is therefore concluded that the raingarden media (and ultimately the K_{sat}) must be decided based on which feature of the raingarden is most important. A solution combining different features, e.g. by having several raingardens/infiltration-based solutions with different infiltration rates in series will add robustness and flexibility.

Acknowledgements

References (including references from appendix)

Ahmed, F., Nestingen, R., Nieber, J. L., Gulliver, J. S. & Hozalski, R. M. 2014. A Modified Philip-Dunne Infiltrometer for Measuring the Field-Saturated Hydraulic Conductivity of Surface Soil. *Vadose Zone Journal,* **13**(10)**,** pp 1-14. DOI: 10.2136/vzj2014.01.0012

Benestad, R. E., Chen, D. & Hanssen-Bauer, I. 2007. *Empirical-Statistical Downscaling*.

Bergen kommune (The Municipality of Bergen). 2005. *Retningslinjer for overvannshåndtering i Bergen (Guidelines for stormwater handling in the Municipality of Bergen)*, Report 11.02.2005, Byrådsavdeling for byutvikling og Vann- og avløpsetaten (City Council for City Development and the Water and Wastewater Agency), The municipality of Bergen, Bergen, Norway.

Brown, C. & Wilby, R. L. 2012. An Alternate approach to Assessing Climate Risks. *Eos, Transactions Amarican Geophysical Union,* **93** (41), pp 401-402. DOI: 10.1029/2012EO410001

Coles, S. 2001. *An Introduction to Statistical Modeling of Extreme Values*, Springer-Verlag, London, UK.

Cunnane, C. 1978. Unbiased plotting positions — A review. *Journal of Hydrology,* **37**(3)**,** pp 205-222.

Dalen, T. 2010. *Hydrologisk dimensjonering av regnbed i kaldt klima (Hydrological Design of Raingardens in cold climate)*. M.Sc. Thesis, Norwegian University of Science and Technology (NTNU), Trondheim, Norway.

Demuzere, M., Orru, K., Heidrich, O., Olazabal, E., Geneletti, D., Orru, H., Bhave, A. G., Mittal, N., Feliu, E. & Faehnle, M. 2014. Mitigating and adapting to climate change: Multi-functional and multi-scale assessment of green urban infrastructure. *Journal of Environmental Management,* **146**, pp107-115.

Dussaliant, A. R., Cuevas, A. & Potter, K. W. 2005. Raingardens for stormwater infiltration and focused groundwater recharge – simulations for different world climates. *Water Science and Technology: Water Supply*, **5**(3), pp 173-179.

Gringorten, I. I. 1963. A plotting rule for extreme probability paper. *Journal of Geophysical Research,* **68**(3), pp 813-814.

Guo, S. L. 1990. A discussion on unbiased plotting positions for the general extreme value distribution. *Journal of Hydrology,* **121**(1-4)**,** pp 33-44.

Hanssen-Bauer, I., Førland, E. J., Haddeland, I., Hisdal, H., Mayer, S, Nesje, A., Nilsen, J. E. Ø., Sandven, S., Sandø, A. B., Sorteberg, A. & Ådlandsvik, B. 2015. *Klima i Norge 2100 (The Climate in Norway 2100)*, Report NCCS no 2/2015, Miljødirektoratet (Norwegian Environment Agency), Norway.

Herath, S. M., Sarukkalige, P. R. & Nguyen, V. T. V. 2016. A spatial temporal downscaling approach to development of IDF relations for Perth airport region in the context of climate change. *Journal Des Sciences Hydrologiques* (*Hydrological Sciences Journal),* **61**(11), pp 2061-2070. DOI: 10.1080/02626667.2015.1083103

Hunt, W. F., Smith, J. T., Jadlocki, S. J., Hethaway, J. M. & Eubanks, P. R. 2008. Pollutant removal and peak flow mitigation by a bioretention call in urban Charlotte, NC. *Journal of Environmental Engineering – Ace*, **134**(5), pp 403-408.

Jonassen, M. O., Olafsson, H., Valved, A. S., Reuder, J. & Olseth, J. A. 2013. Simulations of the Bergen orographic wind shelter. *Tellus A,* **65**. DOI: 10.3402/tellusa.v65i0.19206

Lindholm, O. G. 1987. Følsomhetsanalyse av inngangsparametere i modell for avløpsberegninger. *VANN,* **22**(1)**,** pp. 66-77

Mahmood, R. & Babel, M. S. 2013. Evaluation of SDSM developed by annual and monthly sub-models for downscaling temperature and precipitation in the Jhelum basin, Pakistan and India. *Theoretical and Applied Climatology,* **113**(1), pp 27-44. DOI: 10.1007/s00704-012-0765-0

Makkonen, L. 2008. Problems in the extreme value analysis. *Structural Safety,* **30**(5)**,** pp 405-419.

Mein, R. G. & Larson, C. L. 1973. Modelling infiltration during a steady rain. *Water Resources Research,* **9**(2)**,** pp 384-394. DOI: 10.1029/WR009i002p00384

Nguyen, V. T. V., Desramaut, N. & Nguyen, T. D. 2010. Optimal rainfall temporal patterns for urban drainage design in the context of climate change. *Water Science and Technology,* **62**(5)**,** pp 1170-1176.

Nguyen, V. T. V., Nguyen, T. D. & Ashkar, F. 2002. Regional frequency analysis of extreme rainfalls. *Water Science and Technology,* **45**(2), pp 75-81. DOI: 10.1007/s00704-012-0763-2

Nguyen, V. T. V., Nguyen, T. D. & Cung, A. 2007. A statistical approach to downscaling of sub-daily extreme rainfall processes for climate-related impact studies in urban areas. *Sustainable and Safe Water Supplies,* **7**(2), pp 183-192. DOI: 10.2166/ws.2007.053

Nilsen, V., Lier, J. A., Bjerkholt, J. T. & Lindholm, O. G. 2011. Analysing urban floods and combined sewer overflows in a changing climate. *Journal of Water and Climate Change,* **2**(4)**,** pp 260-271. DOI: 10.2166/wcc.2011.042

Norsk klimaservicesenter (The Norwegian Climate Service Centre). 2016. *Klimaprofil Hordaland (Climate Profile Hordaland)*, Report August 2016, Norway.

Paus, K. H. & Braskerud. B. C. 2014. Suggestions for Designing and Building Bioretention cells for Nordic Conditions. *VATTEN – Journal of Water Management and Research,* **70**(3), pp 139-150.

Paus, K. H., Muthanna, T. M. & Braskerud, B. C. 2016. The hydrological performance of bioretention cells in regions with cold climates: seasonal variations and implications for design. Hydrology Research, **47**(2), pp 291-304.

RStudio Team. 2015. RStudio: Integrated Development Environment for R. RStudio, Inc., Boston, MA. http://www.rstudio.com/

Scholz, F. W. 2006. Maximum Likelihood Estimation. In: *Encyclopedia of Statistical Sciences*. John Wiley & Sons, Inc. DOI: 10.1002/0471667196.ess1571.pub2

Van Genuchten, M. T. 1980. A closed-form equation for predicting the hydraulic conductivity of saturated soils. *Soil Science Society of America Journal,* **44**(5)**,** pp 892-898.

Walter, J. R., Ahlam, S. & Richard, H. M. 1981. Evaluation of Methods for Determining Urban Runoff Curve Numbers. **24**(6)**,** pp. 1562-1566

Wilby, R. L., Dawson, C. W. & Barrow, E. M. 2002. SDSM – a decision support tool for the assessment of regional climate change impacts. *Environmental Modelling & Software,* **17**(2), pp 147-159. DOI: 10.1016/S1364-8152(01)00060-3

Wilby, R. L., Dawson, C. W., Murphy, C., O'Connor, P. & Hawkins, E. 2014. The Statistical DownScaling Model - Decision Centric (SDSM-DC): conceptual basis and applications. *Climate Research,* **61**(3)**,** pp 259-276. DOI: 10.3354/cr01254

Wilby, R. L. & Dessai, S. 2010. Robust adaptation to climate change. *Weather,* **65**(7)**,** pp 180-185. DOI: 10.1002/wea.543

Yahaya, A. S., Nor, N. M. & Jali, N. R. M. 2012. Determination of the Probability Plotting Position for Type I Extreme Value distribution. *Journal of Applied Sciences,* **12**(14)**,** pp 1501-1506.

Yates, D. N., Miller, K. A., Wilby, R. L. & Kaatz, L. 2015. Decision-centric adaptation appraisal for water management across Colorado's Continental Divide. *Climate Risk Management,* **10**, pp 35-50.

Ødegaard, H. 2014. *Vann- og avløpsteknikk (Water and Wastewater Technology),* Norsk Vann, Norway.

Appendix A   The study site
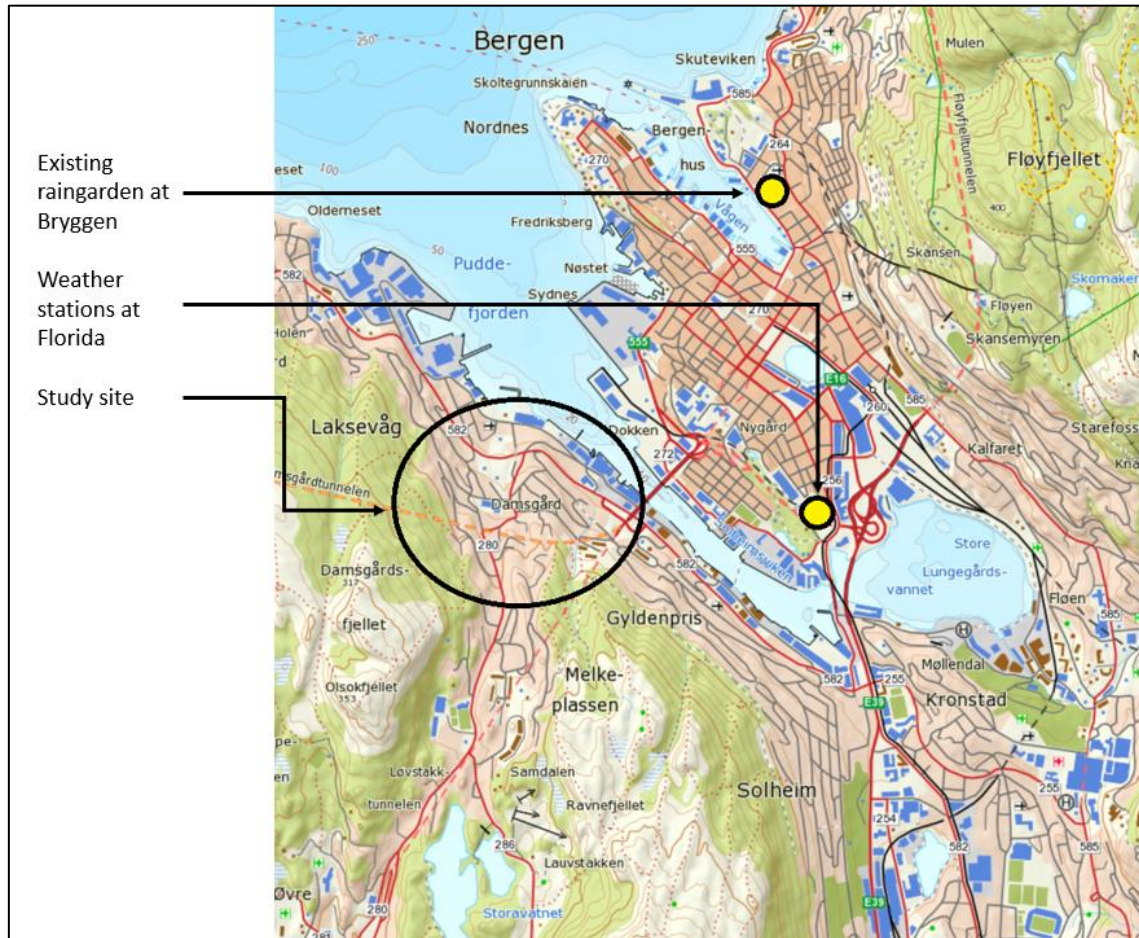
Figure A.1 The study site Damsgård, the existing raingarden at Bryggen and the weather stations at Florida.

Figure A.2 The two weather stations used in the study.

Appendix B   Detailed description of the method

The applied method is described in the paper manuscript. However, a more detailed description of some of the steps follows in the next paragraphs.

B.1. Bias correction

As described by Nguyen *et al.* (2007) and Herath *et al.* (2016), a regression based bias correction method was used to improve the accuracy of the spatially downscaled precipitation. The following equations describe the approach:

$$P_\tau = P_{0\tau} + e_\tau \tag{3}$$

where P_τ is the adjusted daily AM rainfall at the probability level T, $P_{0\tau}$ is the AM rainfall from SDSM and e_τ is the corresponding residual. e_τ was estimated with a second order regression function:

$$e_\tau = aP_{0\tau}^2 + bP_{0\tau} + c + e \tag{4}$$

where a, b and c are parameters of the regression function and e is the resulting error term (see Figure D.1 for the developed bias correction function).

The bias correction was done by developing a script in RStudio, an open source software for the programming language R (RStudio Team 2015). The residual was found for historical data, and the same residual was applied on future precipitation scenarios.

B.1.1. Probability level

To find the probability level T, the Cunnane (Cunnane 1978), Gringorten (Gringorten 1963) and Landwehr (Makkonen 2008) plotting positions were tested. Cunnane and Gringorten have been found to perform well for the GEV distribution (Guo 1990), whereas Landwehr performs well for small samples (Yahaya *et al.* 2012). In this study, they all preformed quite similar. Therefore, the Cunnane plotting position, which gave values between the two others, was chosen for estimating the exceedance probabilities and return levels. The Cunnane plotting position is described by the following equation (Guo 1990):

$$P_i = \frac{i - 0.4}{N + 0.2} \tag{5}$$

where $P_i = \frac{1}{T_i}$ is the plotting (exceedance) probability, i is the rank and N is the sample size.

B.2. Temporal downscaling

The temporal downscaling was conducted as described in Figure B.1.
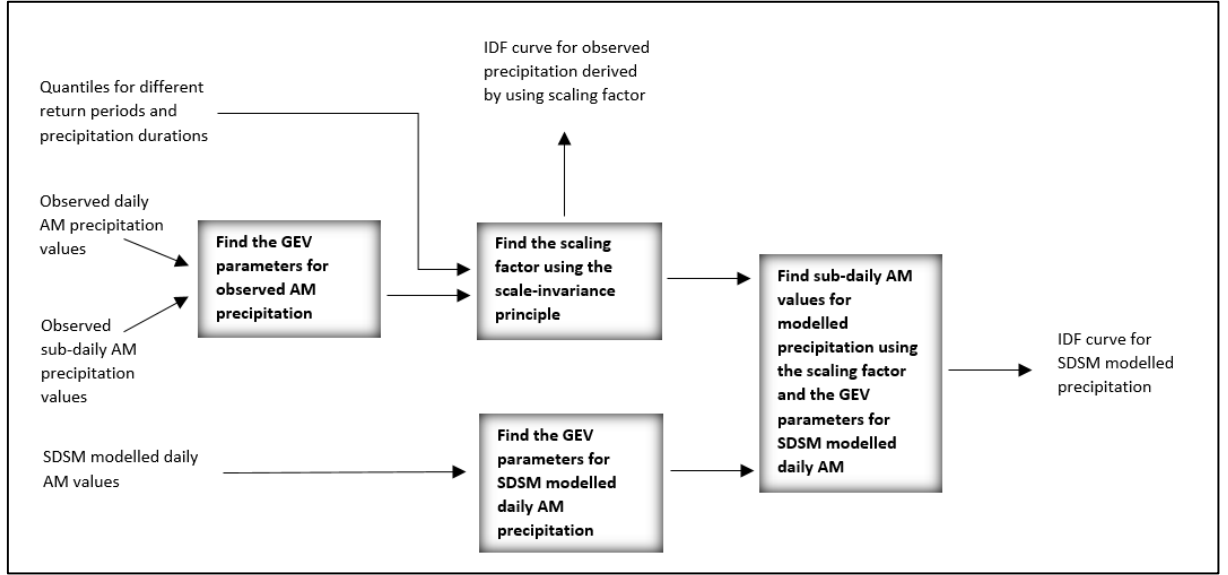
Figure B.1 Flow chart describing the temporal downscaling method.

The GEV distribution was used to model the AM precipitation, as suggested by Nguyen *et al.* (2002). The cumulative distribution function is given as (Coles 2001):

$$G(z) = exp\left\{-\left[1 + \xi\left(\frac{z - \mu}{\sigma}\right)\right]^{-\frac{1}{\xi}}\right\} \tag{6}$$

for $\xi \neq 0$. ξ, μ and σ are the shape, location, and scale parameter respectively.

The GEV parameters were estimated using the MLE method, as described in the paper manuscript. The shape, location and scale parameters were first calculated for the daily precipitation. When calculating the parameters for the other precipitation durations, the shape parameter was fixed to the value of daily precipitation (see Eq. 7).

The concept of scale-invariance, or scaling, applies for the statistical properties of the GEV distribution and hence the relationship between two different time scales t and λt (e.g. daily and sub-daily) can be described as following (Nguyen *et al.* 2002):

$$\xi(\lambda t) = \xi(t) \tag{7}$$
$$\sigma(\lambda t) = \lambda^\beta \sigma(t) \tag{8}$$
$$\mu(\lambda t) = \lambda^\beta \mu(t) \tag{9}$$

$$Z_T(\lambda t) = \lambda^\beta Z_T(t) \tag{10}$$

where β is the scaling factor. The quantiles, Z_T, used for estimating the scaling factors were calculated as (Nguyen 2002):

$$Z_T = \mu + \frac{\sigma}{\xi} \left\{ 1 - [-\log(p)]^\xi \right\} \tag{11}$$

where $p = \frac{1}{T}$ is the exceedance probability.

Scaling factors were calculated from the derived GEV parameters and quantiles using observed historical precipitation (Eq. 7 – Eq. 10). As described in the paper manuscript, they were further plotted against precipitation duration with the aim of finding one common scaling factor. This was calculated by finding the mean of the derived scaling factors.

IDF curves were constructed as described in the paper manuscript. RStudio was used for executing the temporal downscaling (see Appendix F) and for construction of the IDF curves.

B.3. Deciding design duration

Two possible approaches for deciding design duration were considered: (1) Using a duration equal concentration time[1] (Lindholm 1978); and (2) using one-hour events, which often are used for urban drainage network design (Herath *et al.* 2016).

Approach (1) was investigated by calculating the concentration time as recommended by Bergen kommune (2005), using the values in Table B.1 and Figure B.2. From this, a run-on time of approximately three minutes was obtained. However, the shortest duration in the developed IDF curves was 15 minutes (see section 3.3 in the paper manuscript). Therefore, to be able to construct a reasonable precipitation event, a one-hour event (Approach (2)) was used. Since the events were simulated using hyetographs (see section 2.4.4 in paper manuscript), it was ensured that the high-intensity minutes were represented also with Approach (2) (Ødegaard 2014).

---

[1] The concentration time is the time a water molecule spends from the uppermost part of the watershed to the investigated site in the watershed (Bergen kommune 2005).

Table B.1 Values used for calculating concentration time. Watershed characteristics of the existing raingarden at Bryggen were used.

| Variable	Value	Value from/ derived by using
Run-on distance from watershed (m)	120	Google maps' measure function
Slope (‰)	100	Norgeskart.no: 12 m height difference
Runoff coeffisient	0.95	Bergen kommune 2005
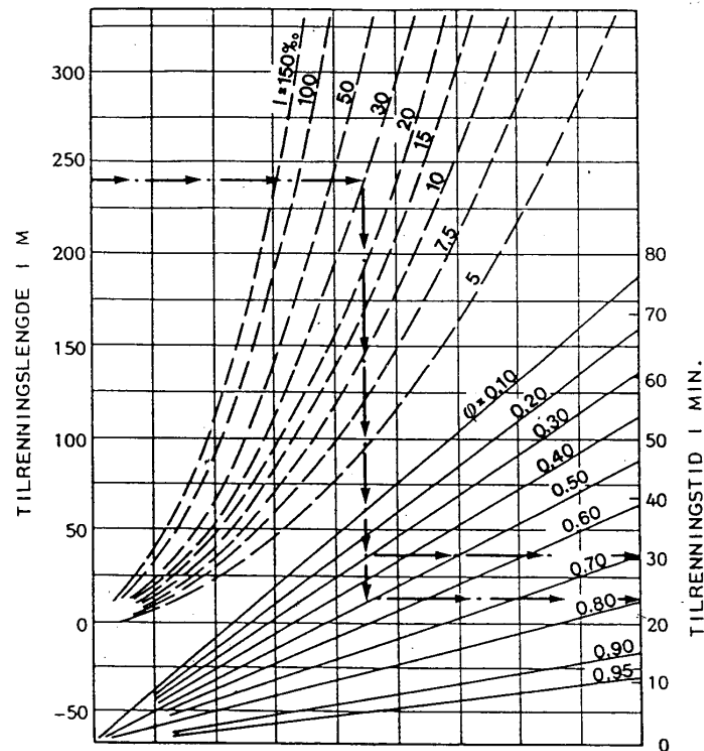
Figure B.2 Nomogram for calculation of concentration time (Bergen kommune 2005).

Appendix C   Simulations in RECARGA

C.1. Input to RECARGA

Table C.1 The input used for the RECARGA simulations. Properties of the existing raingarden at Bryggen, Bergen, were used.

Input type (Abbreviation in the MATLAB code)	Value	Value based on/assumptions
Facility Area (m^2) *Arg*	180.8	Design drawings
Tributary area (m^2) *TribA*	2900	Information from designer
Percent imprevious *EIA*	95	By visual inspection using google maps
CN *CN*	98	The area consists mainly of roads and houses. There are very few gardens. There are (partly) storm sewers. Average soil conditions (AMCII) assumed (Walter *et al.* 1981)
Regional average evapotranspiration *avet*	0	Evapotranspiration is irrelevant for peak flow calculations
Depression zone Depth (cm) *dmin*	12	Design drawings
Root layer Type	2 – fine sand	The root layer consists of 93% sand (from designer)
Saturated hydraulic conductivity (cm/min) *Krz*	0.05667 0.167 0.63	Testing for K_{sat} 3.4 cm/hr, 10 cm/hr and 38 cm/hr
Depth (cm)	38	Design drawings
Storage layer Type	1 – sand	Gravel (design drawings), but sand is the closest to this in RECARGA
Saturated hydraulic conductivity (cm/min) *Kst*	10	Since the media is gravel, a K_{sat} large enough to not delaying was chosen
Depth (cm) *St*	30	Design drawings
Native soil layer Type	10 – clay loam	Closest to actual native soil
Saturated hydraulic conductivity (cm/min) *Kcz*	0.0004167	Native soil has $K_{sat} = 0.25$ cm/hr (from designer)
Depth (cm) *Scz*	0	
Underdrain flowrate (cm/min)	0.338	Calculated automatically by RECARGA from the underdrain diameter
Diameter (m)	0.11	Design drawings

C.2. Comments on the modified version of RECARGA

Before using the version of RECARGA modified by Dalen (2012), the performance of it was assessed by visual inspection of output and comparing to hand calculations and to the results obtained by Dalen (2012). It was found that the results seem reasonable. RECARGA gives however output to a summary file (text file) and to a record file (excel file). It was found that the results in the two output formats differ somewhat. The reason for this might be that the record file output is calculated by fewer decimals than the summary file output. This conclusion was drawn by testing with very low K_{sat} values, giving zero recharge in the record file and a small recharge in the summary file. In this study, the results from the record file was used.

Appendix D   Results

D.1. Spatial downscaling

D.1.1. SDSM

Table D.1 R^2 values for the model.

Month	R^2	Cross validation R^2	% difference between R^2 and cross validation R^2
January	0.23	0.20	13.89
February	0.22	0.21	4.71
March	0.23	0.22	2.92
April	0.22	0.18	16.61
May	0.25	0.24	3.69
June	0.18	0.15	12.81
July	0.11	0.08	30.52
August	0.25	0.25	0.04
September	0.26	0.25	4.60
October	0.23	0.20	11.42
November	0.24	0.19	18.47
December	0.22	0.22	1.53
Mean	0.22	0.20	8.99

D.1.2. Bias correction
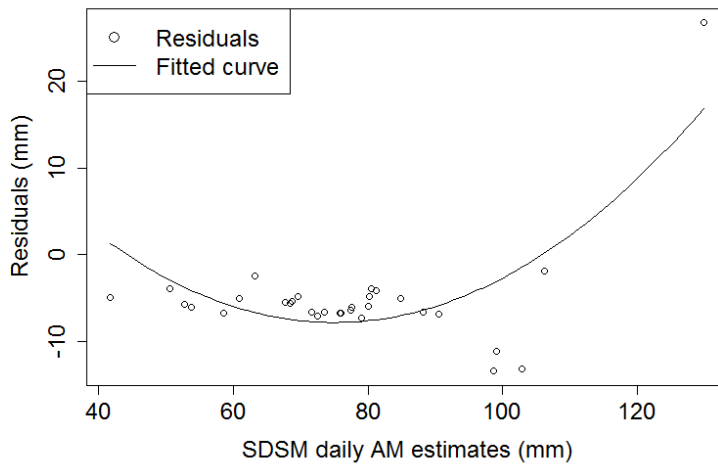
Figure D.1 Bias correction function for daily AM rainfall downscaled with SDSM.

Table D.2 Accuracy of model before and after bias correction.

	Before bias correction	After bias correction
RMSE (mm)	8.14	4.19
N-S (-)	0.85	0.96
p-bias (%)	7.20	8.63e-15

28

D.2. Temporal downscaling

D.2.1. GEV model fit

a) Daily
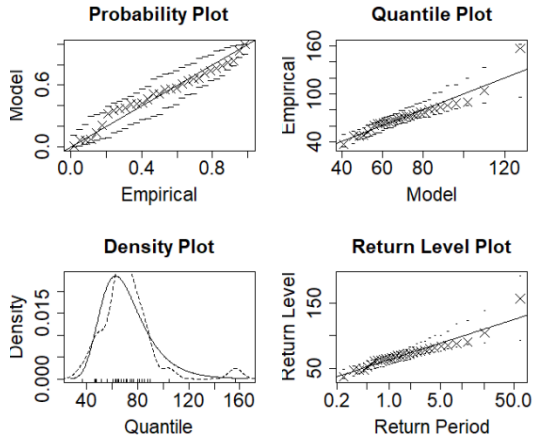
b) 12-hour
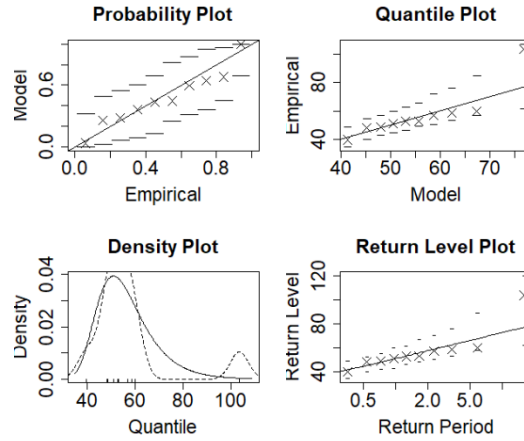
c) 6-hour
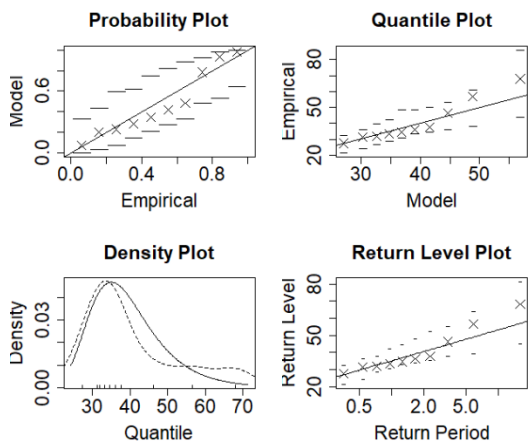
d) 3-hour
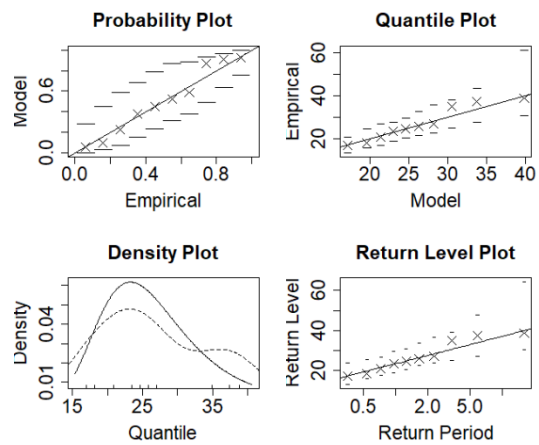
e) 1-hour
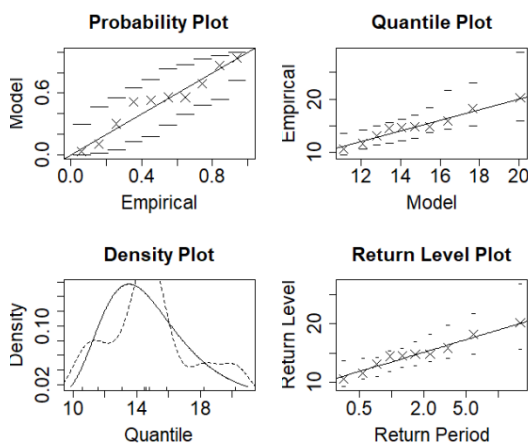
e) 30-minute
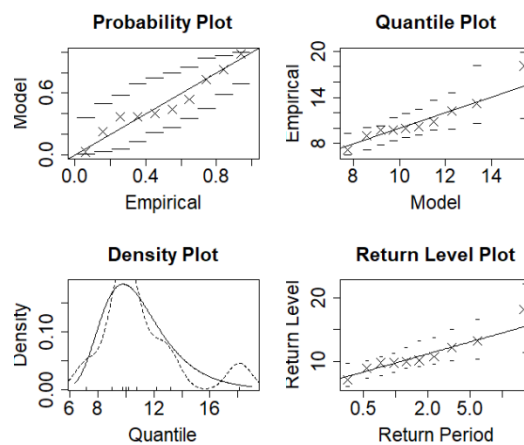
f) 15-minute
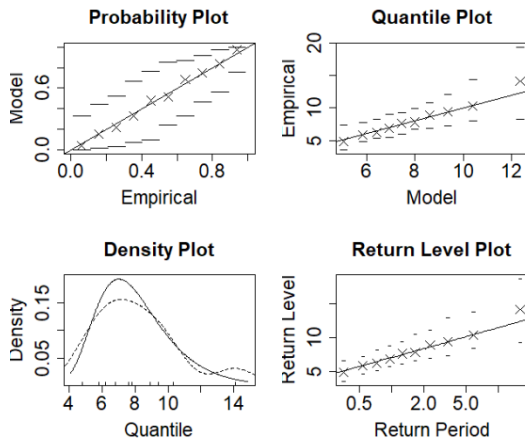
g) 5-minute
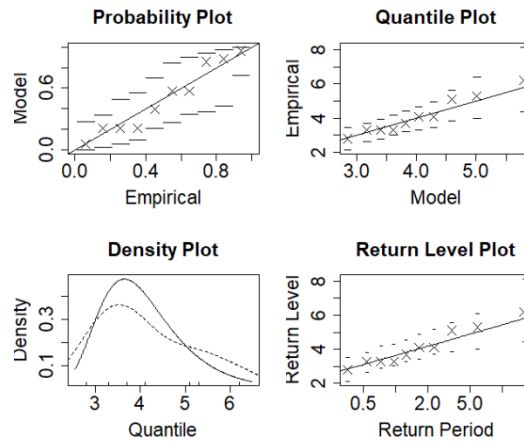
h) 2-minute
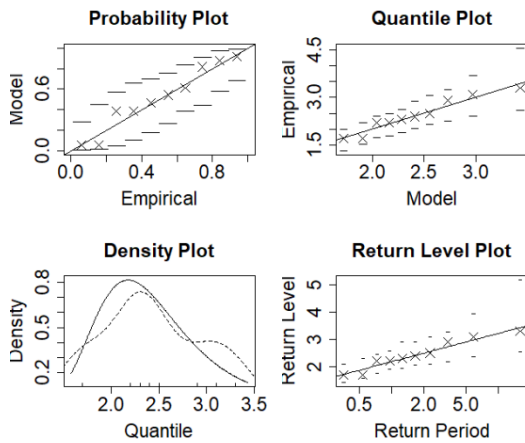
Figure D.2 Summary of GEV fit, as given by the the R package 'evd', for precipitation events with different durations. 'evd' was used for fitting the data to the GEV distribution and finding the GEV parameters, applying MLE. Solid line: GEV model; x and dotted line: observed data; - : the 95th percentile.

D.2.2. Estimation of scaling factors
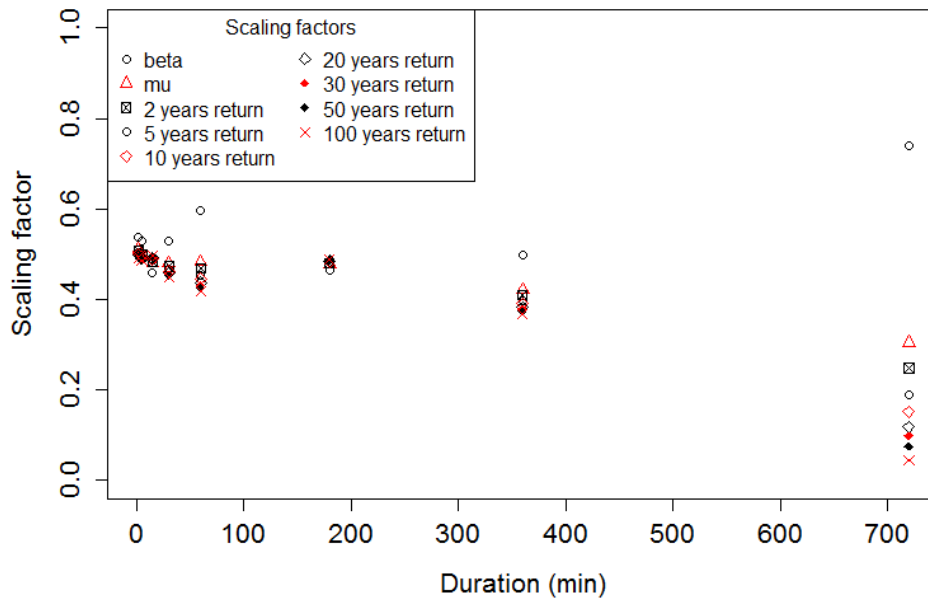
Figure D.3 Scaling factors for statistical properties of the GEV distribution for all durations. As discussed in section 3.3 in the paper manuscript, is the scaling factors for 12-hour duration diverging from the scaling factors for the other durations.
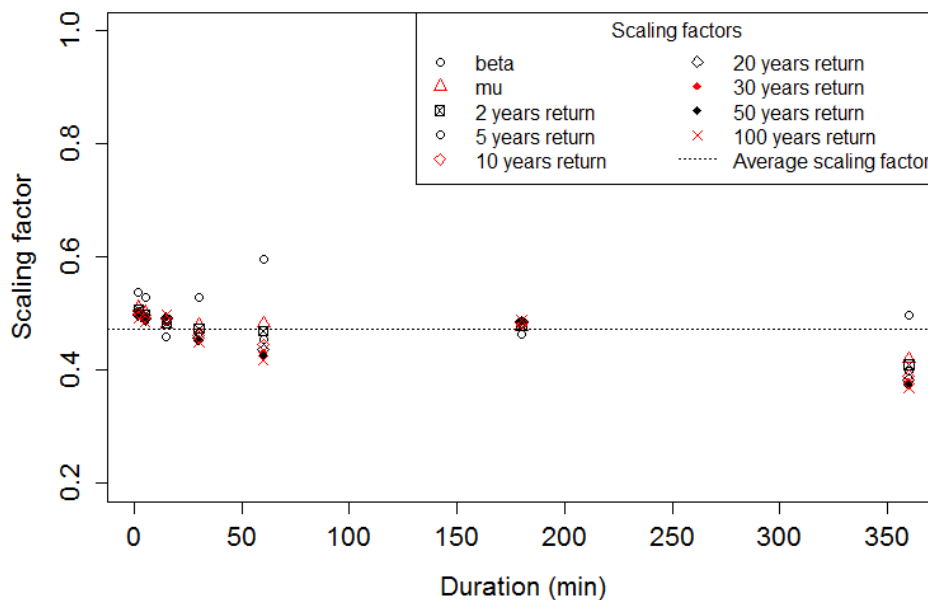

Figure D.4 Scaling factors for statistical properties of the GEV distribution for durations up to 6 hours. The mean of these scaling factors was used to decide one common scaling factor.

Appendix E Poster presented at the conference

Embrace the Water

Read the QR code to find the poster in A0 format. Alternatively, the poster can be found at Daim.

Appendix F Script for deriving the GEV parameters and the scaling factor

The following R script was used for deriving the GEV parameters and the scaling factor. It was combined with the use of other R scripts (which can be found at Daim) to execute the spatial-temporal downscaling.

```r
#GEV PARAMETERS AND SCALING FACTORS
#Guro Heimstad Kleiven, with supervision from Erle Kristvik
#09.03.17, Trondheim
#NONE OF THE INPUT OR OUTPUT OF THIS FILE SHOULD BE CHANGE AS LONG AS THE
#OBSERVED DATA IS THE SAME
setwd("C:/Users/Bruker/OneDrive - NTNU/Masteroppgave/Temporal downscaling")
require("evd")
#Import the AM data for different durations
########################################
min2AM <- read.table('min2AM.txt', header = TRUE)
min5AM <- read.table('min5AM.txt', header = TRUE)
min15AM <- read.table('min15AM.txt', header = TRUE)
min30AM <- read.table('min30AM.txt', header = TRUE)
hr1AM <- read.table('hr1AM.txt', header = TRUE)
hr3AM <- read.table('hr3AM.txt', header = TRUE)
hr6AM <- read.table('hr6AM.txt', header = TRUE)
hr12AM <- read.table('hr12AM.txt', header = TRUE)
dAM <- read.table('DailyObservedAM.txt', header = TRUE)
#Estimate the GEV parameters for different durations
########################################################
#GEV parameters for daily precipitation
##Daily
dGEVfit <- fgev(dAM$AM)                          #Fit the data to the GEV-distribution
dGEVfit
par(mfrow = c(2,2))
plot(dGEVfit)
dpar <- as.numeric(dGEVfit$estimate)             #Get the estimated parameters
dxi <- dpar[3]                                   # xi for daily precipitation
dmu <- dpar[1]                                   # mu for daily precipitation
dbeta <- dpar[2]                                 # beta for daily precipitation
#GEV parameters for the other durations
##2 minutes
min2GEVfit <- fgev(min2AM$AM, shape = dxi)       #Fit data to GEV, with fixed shape
parameter
min2GEVfit
par(mfrow = c(2,2))
plot(min2GEVfit)
```

```r
min2par <- as.numeric(min2GEVfit$estimate)
min2xi <- dxi
min2mu <- min2par[1]
min2beta <- min2par[2]
##5min
min5GEVfit <- fgev(min5AM$AM, shape = dxi)
min5GEVfit
par(mfrow = c(2,2))
plot(min5GEVfit)
min5par <- as.numeric(min5GEVfit$estimate)
min5xi <- dxi
min5mu <- min5par[1]
min5beta <- min5par[2]
##15min
min15GEVfit <- fgev(min15AM$AM, shape = dxi)
min15GEVfit
par(mfrow = c(2,2))
plot(min15GEVfit)
min15par <- as.numeric(min15GEVfit$estimate)
min15xi <- dxi
min15mu <- min15par[1]
min15beta <- min15par[2]
##30min
min30GEVfit <- fgev(min30AM$AM, shape = dxi)
min30GEVfit
par(mfrow = c(2,2))
plot(min30GEVfit)
min30par <- as.numeric(min30GEVfit$estimate)
min30xi <- dxi
min30mu <- min30par[1]
min30beta <- min30par[2]
##1hr
hr1GEVfit <- fgev(hr1AM$AM, shape = dxi)
hr1GEVfit
par(mfrow = c(2,2))
plot(hr1GEVfit)
hr1par <- as.numeric(hr1GEVfit$estimate)
hr1xi <- dxi
hr1mu <- hr1par[1]
hr1beta <- hr1par[2]
##3hr
hr3GEVfit <- fgev(hr3AM$AM, shape = dxi)
hr3GEVfit
par(mfrow = c(2,2))
plot(hr3GEVfit)
hr3par <- as.numeric(hr3GEVfit$estimate)
```

```r
hr3xi <- dxi
hr3mu <- hr3par[1]
hr3beta <- hr3par[2]
##6hr
hr6GEVfit <- fgev(hr6AM$AM, shape = dxi)
hr6GEVfit
par(mfrow = c(2,2))
plot(hr6GEVfit)
hr6par <- as.numeric(hr6GEVfit$estimate)
hr6xi <- dxi
hr6mu <- hr6par[1]
hr6beta <- hr6par[2]
##12hr
hr12GEVfit <- fgev(hr12AM$AM, shape = dxi)
hr12GEVfit
par(mfrow = c(2,2))
plot(hr12GEVfit)
hr12par <- as.numeric(hr12GEVfit$estimate)
hr12xi <- dxi
hr12mu <- hr12par[1]
hr12beta <- hr12par[2]
#Make a matrix of observed GEV parameters (for later use)
ddistpar <- c(dxi, dmu, dbeta)
min2distpar <- c(min2xi, min2mu, min2beta)
min5distpar <- c(min5xi, min5mu, min5beta)
min15distpar <- c(min15xi, min15mu, min15beta)
min30distpar <- c(min30xi, min30mu, min30beta)
hr1distpar <- c(hr1xi, hr1mu, hr1beta)
hr3distpar <- c(hr3xi, hr3mu, hr3beta)
hr6distpar <- c(hr6xi, hr6mu, hr6beta)
hr12distpar <- c(hr12xi, hr12mu, hr12beta)
mdistpar <- matrix(c(ddistpar, min2distpar, min5distpar, min15distpar, min30distpar,
hr1distpar, hr3distpar, hr6distpar, hr12distpar), nrow = 3)
colnames(mdistpar, do.NULL = FALSE)
colnames(mdistpar) <- c('day', '2min', '5min', '15min', '30min', '60min', '180min',
'360min', '720min')
rownames(mdistpar) <- c('xi', 'mu', 'beta')
mdistpar <- as.data.frame(mdistpar)
tmdistpar <- as.data.frame(t(mdistpar))
#Find scaling factors
#########################
#Calculate the quantiles as done by Nguyen et al
Treturn <- c(2, 5, 10, 20, 30, 50, 100)  #return period
p <- 1/Treturn                            #probability
##Daily
dXt <- dmu + (dbeta/dxi)*(1-(1-log(p))^(dxi))
```

35

```r
par(mfcol = c(1, 1))
plot(Treturn, dXt, ylab = "Return level: Daily AM (mm)")
##2 min
min2Xt <- min2mu + (min2beta/min2xi)*(1-(1-log(p))^(min2xi))
par(mfcol = c(1, 1))
plot(Treturn, min2Xt, ylab = "Return level (mm)")
##5 min
min5Xt <- min5mu + (min5beta/min5xi)*(1-(1-log(p))^(min5xi))
par(mfcol = c(1, 1))
plot(Treturn, min5Xt, ylab = "Return level (mm)")
##15 min
min15Xt <- min15mu + (min15beta/min15xi)*(1-(1-log(p))^(min15xi))
par(mfcol = c(1, 1))
plot(Treturn, min15Xt, ylab = "Return level (mm)")
##30 min
min30Xt <- min30mu + (min30beta/min30xi)*(1-(1-log(p))^(min30xi))
par(mfcol = c(1, 1))
plot(Treturn, min30Xt, ylab = "Return level (mm)")
##1 hr
hr1Xt <- hr1mu + (hr1beta/hr1xi)*(1-(1-log(p))^(hr1xi))
par(mfcol = c(1, 1))
plot(Treturn, hr1Xt, ylab = "Return level (mm)")
##3 hr
hr3Xt <- hr3mu + (hr3beta/hr3xi)*(1-(1-log(p))^(hr3xi))
par(mfcol = c(1, 1))
plot(Treturn, hr3Xt, ylab = "Return level (mm)")
##6 hr
hr6Xt <- hr6mu + (hr6beta/hr6xi)*(1-(1-log(p))^(hr6xi))
par(mfcol = c(1, 1))
plot(Treturn, hr6Xt, ylab = "Return level (mm)")
##12 hr
hr12Xt <- hr12mu + (hr12beta/hr12xi)*(1-(1-log(p))^(hr12xi))
par(mfcol = c(1, 1))
plot(Treturn, hr12Xt, ylab = "Return level (mm)")
#Find lambda
durationsMinute <- c(2, 5, 15, 30, 60*1, 60*3, 60*6, 12*60)
durationsHour <- durationsMinute/60
lambda <- durationsHour/24
min2lambda <- lambda[1]
min5lambda <- lambda[2]
min15lambda <- lambda[3]
min30lambda <- lambda[4]
hr1lambda <- lambda[5]
hr3lambda <- lambda[6]
hr6lambda <- lambda[7]
hr12lambda <- lambda[8]
```

```r
##Calculate the scaling factors based on xi, mu, beta, Xt and lambda
###2 min
min2sxi <- 1
min2smu <- (log(min2mu)-log(dmu))/log(min2lambda)
min2sbeta <- (log(min2beta)-log(dbeta))/log(min2lambda)
min2sXt <- (log(min2Xt)-log(dXt))/log(min2lambda)
###5min
min5sxi <- 1
min5smu <- (log(min5mu)-log(dmu))/log(min5lambda)
min5sbeta <- (log(min5beta)-log(dbeta))/log(min5lambda)
min5sXt <- (log(min5Xt)-log(dXt))/log(min5lambda)
###15 min
min15sxi <- 1
min15smu <- (log(min15mu)-log(dmu))/log(min15lambda)
min15sbeta <- (log(min15beta)-log(dbeta))/log(min15lambda)
min15sXt <- (log(min15Xt)-log(dXt))/log(min15lambda)
###30 min
min30sxi <- 1
min30smu <- (log(min30mu)-log(dmu))/log(min30lambda)
min30sbeta <- (log(min30beta)-log(dbeta))/log(min30lambda)
min30sXt <- (log(min30Xt)-log(dXt))/log(min30lambda)
###1 hr
hr1sxi <- 1
hr1smu <- (log(hr1mu)-log(dmu))/log(hr1lambda)
hr1sbeta <- (log(hr1beta)-log(dbeta))/log(hr1lambda)
hr1sXt <- (log(hr1Xt)-log(dXt))/log(hr1lambda)
###3 hr
hr3sxi <- 1
hr3smu <- (log(hr3mu)-log(dmu))/log(hr3lambda)
hr3sbeta <- (log(hr3beta)-log(dbeta))/log(hr3lambda)
hr3sXt <- (log(hr3Xt)-log(dXt))/log(hr3lambda)
###6 hr
hr6sxi <- 1
hr6smu <- (log(hr6mu)-log(dmu))/log(hr6lambda)
hr6sbeta <- (log(hr6beta)-log(dbeta))/log(hr6lambda)
hr6sXt <- (log(hr6Xt)-log(dXt))/log(hr6lambda)
###12 hr
hr12sxi <- 1
hr12smu <- (log(hr12mu)-log(dmu))/log(hr12lambda)
hr12sbeta <- (log(hr12beta)-log(dbeta))/log(hr12lambda)
hr12sXt <- (log(hr12Xt)-log(dXt))/log(hr12lambda)
#Plot the scaling factors
#########################
#Make a matrix of the quantile scaling factors
qsm <- matrix(c(min2sXt,min5sXt,min15sXt,min30sXt,hr1sXt,hr3sXt,hr6sXt,hr12sXt),
              nrow = length(min2sXt))
```

37

```r
colnames(qsm, do.NULL = FALSE)
colnames(qsm) <- c('2min', '5min', '15min', '30min', '60min', '180min', '360min',
'720min')
rownames(qsm) <- c('2', '5', '10', '20', '30', '50', '100')
qsm <- as.data.frame(qsm)
tqsm <- as.data.frame(t(qsm))
#Make a matrix of the scaling factors for the parameters
min2s <- c(min2sxi, min2smu, min2sbeta)
min5s <- c(min5sxi, min5smu, min5sbeta)
min15s <- c(min15sxi, min15smu, min15sbeta)
min30s <- c(min30sxi, min30smu, min30sbeta)
hr1s <- c(hr1sxi, hr1smu, hr1sbeta)
hr3s <- c(hr3sxi, hr3smu, hr3sbeta)
hr6s <- c(hr6sxi, hr6smu, hr6sbeta)
hr12s <- c(hr12sxi, hr12smu, hr12sbeta)
ms <- matrix(c(min2s, min5s, min15s, min30s, hr1s, hr3s, hr6s, hr12s), nrow =
length((min2s)))
colnames(ms, do.NULL = FALSE)
colnames(ms) <- c('2min', '5min', '15min', '30min', '60min', '180min', '360min',
'720min')
rownames(ms) <- c('xi', 'mu', 'beta')
ms <- as.data.frame(ms)
tms <- as.data.frame(t(ms))
xs <- c(2, 5, 15, 30, 60, 180, 360, 720) #The x axis
#Plot the scaling factors
par(mfrow = c(1,1))
plot(xs, tms$beta, ylim = c(0, 1), xlab = 'Duration (min)', ylab = 'Scaling factor',
     cex.axis = 1.3, cex.lab = 1.3)
points(xs, tms$mu, col = 'red', pch = 2)
points(xs, tqsm$`2`, pch = 7)
points(xs, tqsm$`5`, pch = 1)
points(xs, tqsm$`10`, col = 'red', pch = 23)
points(xs, tqsm$`20`, pch = 23)
points(xs, tqsm$`30`, col = 'red', pch = 18)
points(xs, tqsm$`50`,  pch = 18)
points(xs, tqsm$`100`, col = 'red', pch = 4)
legend("topleft", title = 'Scaling factors', pch = c(1, 2, 7, 1, 23, 23, 18, 18, 4),
       col = c('black', 'red', 'black','black', 'red', 'black', 'red', 'black',
'red'),
       c('beta', 'mu', '2 years return', '5 years return', '10 years return', '20
years return',
         '30 years return', '50 years return', '100 years return'), cex = 1, ncol =
2)
##Find the average of the derived scaling factors (excluding 12 hr duration
####because this point is diverging from the rest)
```

```r
sfactors1 <- c(min2smu, min2sbeta, min5smu, min5sbeta, min15smu, min15sbeta,
min30smu, min30sbeta, hr1smu, hr1sbeta, hr3smu, hr3sbeta, hr6smu, hr6sbeta,
tqsm$`2`[1:7],
              tqsm$`5`[1:7], tqsm$`10`[1:7], tqsm$`20`[1:7], tqsm$`30`[1:7],
tqsm$`50`[1:7], tqsm$`100`[1:7])
sfactor <- mean(sfactors1)
xs2 <- xs[1:7]
#Plot the scaling factors and the average. 12 hr duration is excluded
par(mfrow = c(1,1))
plot(xs2, tms$beta[1:7], ylim = c(0.2, 1), xlab = 'Duration (min)', ylab = 'Scaling
factor', cex.axis = 1.3, cex.lab = 1.3)
points(xs2, tms$mu[1:7], col = 'red', pch = 2)
points(xs2, tqsm$`2`[1:7], pch = 7)
points(xs2, tqsm$`5`[1:7], pch = 1)
points(xs2, tqsm$`10`[1:7], col = 'red', pch = 23)
points(xs2, tqsm$`20`[1:7], pch = 23)
points(xs2, tqsm$`30`[1:7], col = 'red', pch = 18)
points(xs2, tqsm$`50`[1:7],  pch = 18)
points(xs2, tqsm$`100`[1:7], col = 'red', pch = 4)
abline(a = sfactor, b = 0, lty = 3)
legend("topright", title = 'Scaling factors', pch = c(1, 2, 7, 1, 23, 23, 18, 18, 4,
NA), lty = c(NA, NA, NA, NA, NA, NA, NA, NA, NA, 3), col = c('black', 'red',
'black','black', 'red', 'black', 'red', 'black', 'red', 'black'),
       c('beta', 'mu', '2 years return', '5 years return', '10 years return', '20
years return', '30 years return', '50 years return', '100 years return', 'Average
scaling factor'), cex = 1, ncol= 2)

#Export the GEV parameters and scaling factor for further use
################################################################
write.table(tmdistpar, file = "Observed GEV parameters.txt", row.names = TRUE,
col.names = TRUE)
write.table(sfactor, file = "Scaling factor.txt")
```